Turk J Phys
36 (2012) , 99 – 107.

doi:10.3906/fiz-1103-1

Coupled-channels analysis of K^+ scattering from ^{6}Li

Ahmed Aly EBRAHIM
Physics Department, Assiut University, Assiut 71516, EGYPT
e-mail: aebrahim@aun.edu.eg

Received: 02.03.2011

Abstract

Differential cross sections for the elastic and inelastic scattering of K^+ at 715 MeV/c from ^{6}Li are analysed by applying the Watanabe superposition model to the real potential with a phenomenological imaginary potential. The optical potential of ^{6}Li is calculated in terms of alpha-particle and deuteron or triton and helion optical potentials. The calculated cross sections are consistent with the triton-helion model.

Key Words: K^+-nucleus reactions, coupled-channels Born approximation, cluster model

PACS: 25.80.Nv, 24.10.Eq, 24.10.Ht

1. Introduction

The procedure given by Satchler [1] states that the relativistic Klein-Gordon equation can be reduced to the non-relativistic Schrödinger equation by redefining the mass and energy of the incident kaons. K^+-nucleus scattering has been studied in this work within the framework of the WS local optical model.

Earlier studies of elastic scattering of K^+ from ^{12}C and ^{40}Ca produced cross sections larger than the predictions of optical model theories [2]. Total cross sections for K^+ mesons on several nuclei at a range of kaon lab momenta also exceeded model expectations [3, 4], which indicates that the behaviour of the nucleons within the nuclear medium is different than that in free space. These observations raised several suggestions on how to overcome this problem. The interesting suggestion is that medium modifications such as nuclear swelling or meson mass scaling might be responsible for disagreement with experimental data. Siegel et al. [4] proposed that the modification of the S11 K^+ scattering amplitude by altering the effective nucleon size in the nucleus. They concluded that an increase of 10–20% in the S11 phase shift markedly improved their agreement with data above 720 MeV/c. Such increase is in line with the estimates of Close et al. [5] on the change of confinement scale in nuclei.

Angular distributions of the elastic scattering cross sections of K^+ on ^{6}Li, ^{12}C and ^{40}Ca at 635, 715 and 800 MeV/c kaon lab momenta were analyzed [6] using the distorted wave Born approximation (DWBA) with DWUCK4 code. The local optical potential of Johnson and Satchler [7] occurred to need enhancement

in the dominated S11 K^+N phase shifts by 10% for low-density ^{6}Li, but 11–12% was required for ^{12}C and ^{40}Ca nuclei. This modification results in better fitting to the experimental data. Increasing the K^+ phase shifts increases the nucleon size; a "swelling" of the nucleon in nuclear medium. This means that the K^+N interaction inside a nucleus will differ from the free space. Moreover, the local optical potential was also used to estimate quadrupole non-central contributions to elastic K^+ scattering from the 1^+ ground state of ^{6}Li, these calculations make no difference to data, but only gave small contributions to monopole for ^{6}Li at large angles. Thus, the 1^+ spin of ^{6}Li can be ignored, and the data can be treated in the same way as the case for zero-spin ^{12}C and ^{40}Ca nuclei. It was concluded that the K^+ data and the elastic calculations show a much less distinct diffraction pattern than is seen for the strongly absorbed pions. This is expected for scattering from a repulsive potential. The same enhancement in S11 K^+N phase shift was required for both elastic and inelastic scattering of K^+ at a certain energy from ^{6}Li or ^{12}C nuclei, while a larger enhancement of S11 K^+N for σ_{tot} and σ_R for both light and heavy nuclei was required. Finally, we concluded that our results from this previous work, which was based on the distorted wave Born approximation (DWBA), in addition to suggestions about nucleon swelling [8], along with calculations based on the impulse approximation, as well as pion excess in nuclei [9, 10], show the possibility of observing some unusual phenomena in K^+-nucleus interaction.

Elastic and inelastic scattering of K^+ from ^{6}Li, ^{12}C and ^{40}Ca in the momentum range 635–800 MeV/c were well reproduced by a six-parameter optical model using the Woods-Saxon shape for both the real and imaginary parts of the potential. The strong absorption radius and σ_R were found to be quite stable over the wide range of parameters [11]. Volume integrals of the resulting potentials showed the expected non-resonant behavior for K^+ scattering as the energy is varied.

The analysis of elastic and inelastic-scattering data can be performed using the folding model in the framework of the distorted-wave Born approximation (DWBA) with DWUCK4 code or coupled channels (CC) with CHUCK code [12]. The program CHUCK calculates nuclear reaction cross sections by numerically solving an appropriate set of coupled equations. In DWBA the distorted wave functions for the incoming and outgoing particles are generated using the optical potential, which describes elastic scattering and the effect of the non-elastic channels is taken into account through the imaginary part of the optical potential. If, however, one or more inelastic channels are strongly coupled to the elastic channel it is not sufficiently accurate to take them into account through the optical potential when calculating the elastic scattering, nor is it sufficiently accurate to use DWBA to calculate the scattering into these inelastic channels [13]. In the CC approximation, as in DWBA, there are essentially no free parameters except those which occur in the model chosen for the nuclear wave functions. The CC mechanism has the additional and very important feature that the wave functions for elastic and inelastic scattering are calculated simultaneously. Both DWBA and CC calculations were carried out [14] for the data of 210 MeV ^{6}Li elastic and inelastic scattering from ^{12}C, ^{28}Si and ^{58}Ni, based on the collective-model description of the first-excited (2^+) states of the target nuclei. Unique ^{6}Li phenomenological optical model potentials were used in these calculations [14].

The main purpose of the present work is to construct a potential model by applying the Watanabe superposition procedure to the real potential with a phenomenological Woods-Saxon imaginary potential, to carefully describe the elastic and inelastic scattering of K^+ leading to the lowest 3^+ state in ^{6}Li at 715 MeV/c and to reduce the ambiguity of the parameters. The alpha-deuteron and triton-helion cluster models for ^{6}Li

nucleus of binding energies 1.47 and 15.7 MeV, respectively, are used. The resulting differential cross sections are compared with the experimental data as well as the phenomenological calculations.

2. Analysis

The elastic and inelastic scattering differential cross sections of K^+ from ^{6}Li are calculated using the coupled-channels code CHUCK. The present calculations have been performed using the phenomenological optical model of Woods-Saxon form and Watanabe superpositions model. The phenomenological Woods-Saxon local potentials can be written as

$$U(r) = -V_0\ f(r) - i\ W_I\ g(r), \tag{1}$$

where

$$f(r) = (1+\exp[(r-R_0)/a_0])^{-1}, \quad g(r) = (1+\exp[(r-R_I)/a_I])^{-1},$$

$$R_i = r_i\ A_{\rm T}^{1/3}, \quad (i = 0, I),$$

r_i and a_i are radius and diffuseness parameters, respectively, and $A_{\rm T}$ is the target mass number.

The coupled-channels code CHUCK calculates the Coulomb and nuclear form factors as

$$F_L(r) = F_L^C(r)\ +\ F_L^N(r) \tag{2}$$

where

$$\begin{aligned} F_L^C(r) &= \frac{3Z_K Z_T}{2L+1}\ \beta_L^C\ \frac{R_{\rm c-ex}^L}{r^{L+1}} && \text{for } r \geq R_{\rm c-ex}, \\ &= 0 && \text{for } r < R_{\rm c-ex}, \end{aligned} \tag{3}$$

with deformed charge radius $R_{\rm c-ex} = r_{0c}\ A_T^{1/3}$ and

$$F_L^N(r) = -\beta_L^N({\rm Re})\ R_0\ V_0\ \frac{df(r)}{dr}\ -\ i\,\beta_L^N({\rm Im})\ R_I\ W_I\ \frac{dg(r)}{dr}, \tag{4}$$

Here $\beta_L^N({\rm Re})$ and $\beta_L^N({\rm Im})$ are the deformation parameters associated with the real and absorptive parts of the nuclear potential $U(r)$, β_L^C is the deformation parameter for the Coulomb potential and Z_T and Z_K are the charges of the target and projectile, respectively. Kinematic factors for use in a non-relativistic Schrödinger equation used in the present work is taken from reference [15]. The nuclear potential $U(r)$ as well as the Coulomb potential are obtained from the fits of the elastic scattering data. The Coulomb potential used here is due to the uniform charge distribution of the target nucleus of radius $R_c = r_{0c}\ A^{1/3}$, where $r_{0c} = 1.2$ fm; see [15] and references therein.

On the basis of the Watanabe superpositions model, the optical potential of ^{6}Li target is expressed in terms of the triton and helion potentials as follows [16]:

$$U_{^6_{Li}}(r) = U_{\rm t-folded}(r)\ +\ U_{\rm h-folded}(r), \tag{5}$$

where

$$U_{\mathrm{t(h)-folded}}(r) = U_{\mathrm{t(h)}}(r) + \frac{7}{72\,\gamma}\left(\frac{d^2U_{\mathrm{t(h)}}(r)}{dr^2} + \frac{2}{r}\frac{dU_{\mathrm{t(h)}}(r)}{dr}\right),$$

with $\gamma = 0.21$ fm^{-1} [17]. Here, U_{t} and U_{h} are the phenomenological optical potentials for triton and helion particles, respectively. The potential for ^{6}Li target can be expressed in terms of alpha-particle and deuteron potentials as [16]:

$$U^{6}_{\mathrm{Li}}(r) = U_{\alpha-\mathrm{folded}}(r) + U_{\mathrm{d-folded}}(r), \tag{6}$$

where

$$U_{\alpha-\mathrm{folded}}(r) = U_{\alpha}(r) + \frac{7}{144\,\beta}\left(\frac{d^2U_{\alpha}(r)}{dr^2} + \frac{2}{r}\frac{dU_{\alpha}(r)}{dr}\right)$$

$$U_{\mathrm{d-folded}}(r) = U_{d}(r) + \frac{7}{36\,\beta}\left(\frac{d^2U_{\mathrm{d}}(r)}{dr^2} + \frac{2}{r}\frac{dU_{\mathrm{d}}(r)}{dr}\right)$$

where β=0.1989 fm^{-2} [18]. U_{α} and U_{d} are the phenomenological optical potentials for alpha and deuteron particles, respectively.

3. Results and discussion

The coupled-channels calculations have been performed using the computing program CHUCK. The radial integrations have been carried out to 40 fm in 0.1 fm steps to account properly for Coulomb excitations. The calculations have been done by coupling, individually, one state to the ground state for all cases under consideration. The phenomenological optical potential for K^+ - ^{6}Li scattering given in Table 1 is used in the present calculations [11]. The Coulomb and nuclear deformation lengths used in the present calculations are δ_3^C =1.72 fm and δ_3^N =1.749 fm. Expressions (2)–(4) together with the parameters given in Table 1 yield the Coulomb and nuclear deformation parameters used in the present calculations are β_3^C =0.705, β_3^N (Re) = 0.875 and β_3^N (Im)=0.655.

Table 1. Woods-Saxon optical potential parameters for ^{6}Li at 715 MeV/c. A positive real potential is attractive and a positive imaginary potential is absorptive.

Reaction	set	V_0 (MeV)	r_0 (fm)	a_0 (fm)	W_{I} (MeV)	R_{I} (fm)	a_{I} (fm)	χ^2	σ_{R} (mb)
$K^+ - {}^{6}$Li	1	13.098	1.100	0.713	19.762	0.7999	0.5715	3.305	63.51
	2	7.429	1.155	0.753	30.003	0.6615	0.6719	3.922	87.74
	3	2.094	1.145	0.953	32.276	0.6453	0.6952	4.413	94.84
	4	−3.397	1.1075	0.6115	25.569	0.7613	0.6355	4.832	83.68

The Watanabe potentials for ^{6}Li in terms of the triton and helion or alpha-particle and deuteron given by expressions (4) or (5) are used to calculate the angular distributions of K^+ scattering from ^{6}Li at 715 MeV/c.

Here, $U_{\rm t}, U_{\rm h}, U_{\alpha}$ and $U_{\rm d}$ included in expressions (5) and (6) are taken as the Woods-Saxon phenomenological potentials given in Table 2. These potentials are chosen from several sets of optical potentials for the triton, helion, alpha-particle and deuteron potentials; these given sets are selected according to the most minimum values of χ^2 and production of the most reasonable fits to the inelastic scattering data. The potentials used here are of the largest diffuseness of the available potentials where the errors due to Tailor expansions used in deriving expressions (5) and (6) are expected to be minimum [19].

Table 2. The optical potential parameters and the associated deformation parameters for the triton, helion, alpha-particle and deuteron used in the Watanabe predictions shown in Figures 1 and 2.

Reaction	V_0 (MeV)	r_0 (fm)	a_0 (fm)	β_3^N (Re)
K^+-t	15.2	1.42	0.717	0.842
K^+-h	13.4	1.35	0.853	0.898
K^+-α	12.9	1.45	0.735	0.735
K^+-d	10.7	1.32	0.45	0.815

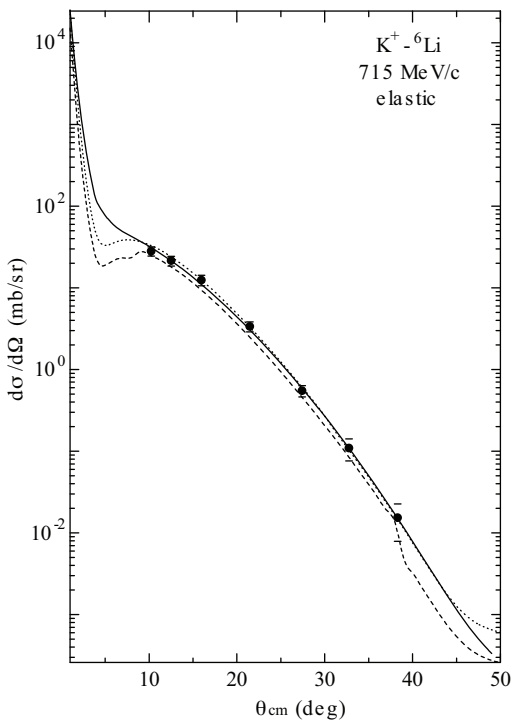

Figure 1. Data for differential elastic cross section scattering at 715 MeV/c K^+ from ^{6}Li [20], compared with the WS optical model parameters set 1 of Table 1 (the solid curve), the triton-helion (the dotted curve) and alpha-deuteron (the dashed curve) Watanabe potentials of expressions (5) and (6) with the parameters given in Table 2 for the real potential.

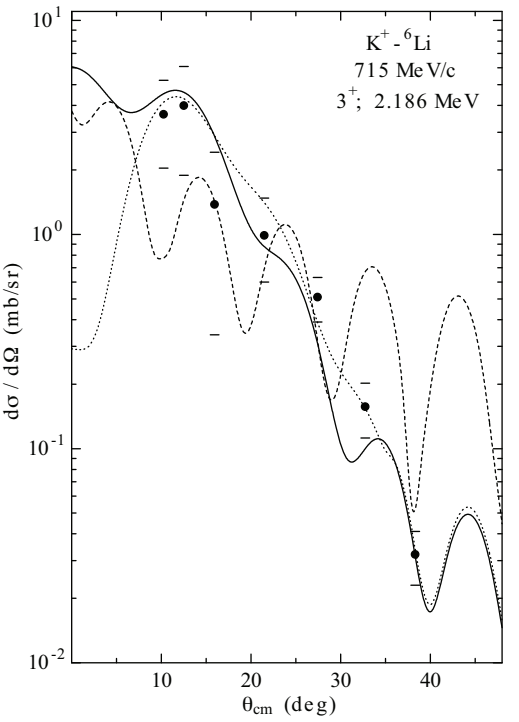

Figure 2. The same as Figure 1, but for the inelastic scattering cross section of K^+ to the 2.186 MeV 3^+ state of ^{6}Li. The experimental data are taken from reference [20].

The real part of ^{6}Li potential calculated by expressions (5) or (6) together with the imaginary part of the ^{6}Li potential given in Table 1 are used to calculate the differential cross sections for K^{+} - ^{6}Li scattering. The resulting angular distributions for the elastic scattering and inelastic scattering to the 3^{+} state in ^{6}Li are shown in Figures 1 and 2, respectively, compared with the experimental data [20] and the predictions of the phenomenological optical potential given in Table 1. In the case of using the Watanabe potentials of expressions (5) or (6), the deformation parameters of the real potential are chosen so that the deformation lengths equal the deformation length of the real phenomenological potential. This yields the associated deformation parameters for the triton, helion, alpha-particle and deuteron potentials and are given in Table 2.

Figures 1 and 2 show fair agreement between the predicted differential cross sections using the Watanabe potential and the experimental data at 715 MeV/c. The Watanabe potential predictions oscillate around the experimental data. Such oscillations are stronger than the oscillation present in the experimental data and in the phenomenological predictions. This is due to the fact that expressions (5) and (6) with the parameters of $U_{\mathrm{t(h)}}$, U_{α} and U_{d} given in Table 2 do not predict well the imaginary potential for ^{6}Li, since the inelastic scattering is sensitive to the choice of scattering potential. In these figures, the cross sections calculated with the triton-helion model of ^{6}Li (as the dotted curves) are in good agreement with the experimental data and the phenomenological calculations using set 1 (the solid curves). The cross sections calculated using the alpha-deuteron model (the dashed curves) agree fairly with elastic data and rather poorer agreement is obtained for the inelastic data at 715 MeV/c.

The K^{+} - ^{6}Li WS local potentials using set 1 in Table 1 (the solid curves), the triton-helion potential model of ^{6}Li (the dotted curves) and the alpha-deuteron potential model (the dashed curves) are shown in Figure 3 at 715 MeV/c. They have one feature in common: the tails of the imaginary potentials are almost identical. The agreement in the interior region is poor. It seems that this region of potential models slightly participates in the elastic scattering mechanism. This result is similar to that of nucleus-nucleus [21] and pion scattering [1, 22, 23]. From that figure it is seen that in this case the real/imaginary part is quite shallow and everywhere attractive/absorptive. The imaginary part is deeper and rapidly decreasing while the real part is shallower and wider. This behavior for both parts of potential is observed for all potential models. These relative shallow potentials for positive kaons compared to those for nucleons and pions confirm that K^{+} mesons weakly interact with nuclei.

Table 3 shows the predictions of the CHUCK code used in the present work for the partial wave angular momentum $L_{1/2}$ corresponding to the strong absorption radius D. The calculated values of this program for the real J_{R} and imaginary J_{I} volume integrals per nucleon of the target nucleus, the Re $U(D)$ and Im $U(D)$ nuclear parts of potential at the distance D and the root mean square radii of the real $<r^{2}>_{\mathrm{R}}^{1/2}$ and imaginary $<r^{2}>_{\mathrm{I}}^{1/2}$ parts of the nuclear potential are also shown in Table 3. It is well known that at the strong absorption radius D the incident particle has a 50% probability of being absorbed by the target nucleus. The strong absorption radius D can be calculated from $L_{1/2}$ using the relation

$$k\,D = [L_{1/2}\,(L_{1/2} + 1) + \eta^{2}]^{1/2} + \eta, \quad \eta = Z_{K} Z_{T}\, e^{2}\, \mu/\hbar^{2}\, k,$$

where η, μ and k are the Sommerfeld parameter, reduced mass and center-of-mass wave number, respectively.

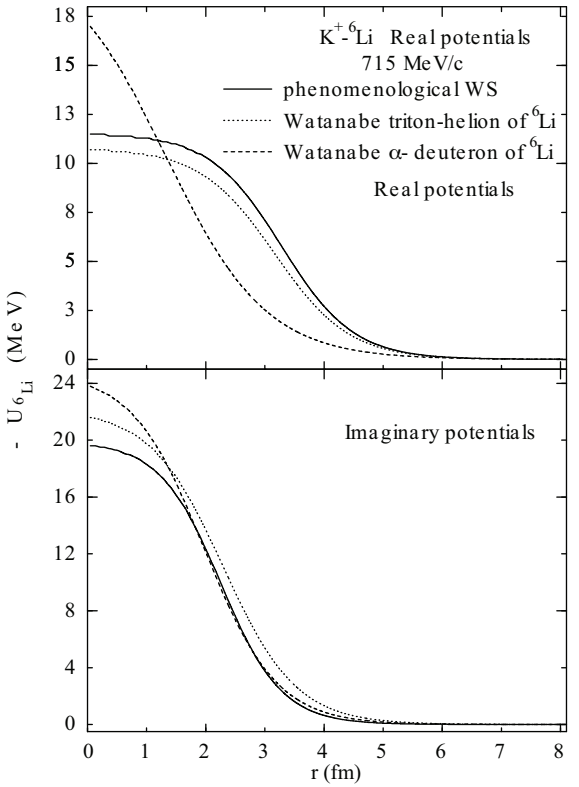

Figure 3. WS optical potentials computed at 715 MeV/c K^+ from ^{6}Li with the parameter set 1 of Table 1 compared with the triton-helion and alpha-deuteron Watanabe potentials of expressions (5) and (6) with the parameters given in Table 2 for the real potential. The solid curves are for the WS potentials, the dotted curves for the triton-helion model and dashed curves for the alpha-deuteron model.

Table 3. Derived quantities for K^+ scattering at 715 MeV/c, using the phenomenological WS parameters (set 1) in Table 1 and parameters of the triton-helion and the alpha-deuteron models in Table 2.

Reaction	$L_{1/2}$	D (fm)	J_R (MeV fm^3)	J_I (MeV fm^3)	Re $U(D)$ (MeV)	Im $U(D)$ (MeV)	$<r^2>_R^{1/2}$ (fm)	$<r^2>_I^{1/2}$ (fm)
K^+-^{6}Li	5.64	2.316	141.55	92.197	10.13	11.43	3.07	2.44
K^+-t	3.42	2.005	70.25	127.06	6.452	9.154	2.55	2.42
K^+-h	3.54	2.009	65.29	125.56	5.754	8.125	2.57	2.45
K^+-α	4.26	2.256	95.62	145.36	7.187	14.35	2.98	2.69
K^+-d	2.94	1.775	52.64	105.46	3.258	8.257	2.35	2.09

From Table 3, it is clear that $<r^2>_R^{1/2}$ is greater than $<r^2>_I^{1/2}$ and both of them are greater than D and the imaginary volume integrals J_I per nucleon of the target nucleus are greater than the real J_R for all cases under consideration. Re $U(D)$ and Im $U(D)$ given in Table 3 for all considered cases show that the drop of the real part of the potential, with respect to V_0 for each potential model, is much less than that of the imaginary part with respect to W_I at the same distance D. This behavior is also reflected by Figure 3.

The CHUCK code using the present potentials predicts the total and reaction cross sections of kaon

scattering on d, t, h, α and ^{6}Li at kaon lab momentum 715 MeV/c. It can be seen from Table 4 that $\sigma_{\rm tot}$ and $\sigma_{\rm R}$ increase as the mass number of target nucleus increases. Low values of $\sigma_{\rm tot}$ shown in Table 4, compared to the corresponding values for pion scattering [24, 25], indicate longer mean free path for K^{+}.

Table 4. Reaction and total cross section values (in mb) for K^{+} interaction with various nuclei calculated at 715 MeV/c.

Nucleus	d	t	h	α	^{6}Li
$\sigma_{\rm R}$	20.42	33.14	37.12	54.27	63.51
$\sigma_{\rm tot}$	28.85	43.42	46.31	65.21	88.05

4. Conclusion

Angular distributions of K^{+} elastically scattered from ^{6}Li at kaon lab momentum 715 MeV/c are more consistent with the triton-helion model, where the binding energy is more than ten times of the binding energy in case of the alpha-deuteron model. The strong absorption radius and $\sigma_{\rm R}$ are found to be quite stable over the wide range of parameters. Volume integrals of the resulting potentials show the expected non-resonant behavior for K^{+} scattering from nuclei.

Inelastic scattering of K^{+} leading to the lowest 3^{+} state in ^{6}Li was then analyzed using CHUCK code. Angular distributions were reasonably well accounted for by the triton-helion potential model produced from the corresponding elastic scattering, without readjustment of any of the parameters. Deformation parameters were extracted. Forcing these to agree with known results provided a resolution of the ambiguity found from elastic fitting only. It can be concluded that, this simple triton-helion potential model of ^{6}Li is effective for K^{+}-nucleus scattering without modifications in-medium K^{+}-nucleon cross sections or other improvements as found with free-space K^{+}-nucleon.

Acknowledgment

I would like to thank Professor R. J. Peterson, University of Colorado at Boulder, for a careful reading of the manuscript.

References

[1] G. R. Satchler, *Nucl. Phys.*, **A540**, (1992), 533.

[2] D. Marlow, *Phys. Rev.*, **C25**, (1982), 2619.

[3] M. F. Jiang, D. J. Ernst, and C. M. Chen, *Phys. Rev.*, **C51**, (1995), 857.

[4] P. B. Siegel, W. B. Kaufmann and W. R. Gibbs, *Phys. Rev.*, **C31**, (1985), 2184.

[5] F. E. Close, R. L. Jaffe, R. G. Roberts and G. G. Ross, *Phys. Rev.*, **D31**, (1985), 1004.

[6] A. A. Ebrahim and S. A. E. Khallaf, *Phys. Rev.*, **C66**, (2002), 044614.

[7] M. B. Johnson and G. R. Satchler, *(Ann. Phys. N. Y.)*, **248**, (1996), 134.

[8] R. J. Peterson, A. A. Ebrahim and H. C. Bhang, *Nucl. Phys.*, **A625**, (1997), 261.

[9] M. F. Jiang and D. Koltum, *Phys. Rev.*, **C46**, (1992), 2462.

[10] S. V. Akulinichev, *Phys. Rev. Lett.*, **68**, (1992), 290.

[11] A. A. Ebrahim and S. A. E. Khallaf, *J. Phys.*, **G30**, (2004), 8395.

[12] P. D. Kunz, CHUCK computer code, University of Colorado, USA (unpublished).

[13] D. F. Jackson, Nuclear Reactions, (Chapman and Hall, London, 1975).

[14] A. Nadasen, M. McMaster, M. Fingal, J. Tavormina, J.S. Winfield, R. M. Ronningen, P. Schwandt, F.D. Becchetti, J. W. Janecke, R. E. Warner, Phys. Rev. **C40**, (1989), 1237.

[15] S. A. E. Khallaf and A. A. Ebrahim, *Phys. Rev.*, **C62**, (2000), 024603.

[16] S. A. E. Khallaf, A.L. Attar and M. F. El-Azab, VII th International Congress on Mathematical Physics, Boulder, Colorado, USA, 1-10 August 1983.

[17] J. C. Bergstrom, *Nucl. Phys.*, **A327**, (1979), 458.

[18] Y. Fujiwara and Y. C. Tang, *Phys. Rev.*, **C27**, (1983), 2457.

[19] G. Madurga, *J. Phys.* **G9** (1983), L 279.

[20] R. E. Chrien, R. Sawafta, R. J. Peterson, R.A. Michael and E. V. Hungerford, *Nucl. Phys.*, **A625**, (1997), 251.

[21] Bikash Sinha, *Phys. Rev.*, **C11**, (1975), 1546.

[22] E. Friedman et al., *Phys. Rev.*, **C72**, (2005), 034609.

[23] M. Döring, E. Oset, *Phys. Rev.*, **C77**, (2008), 024602.

[24] S. A. E. Khallaf and A. A. Ebrahim, *Phys. Rev.*, **C65**, (2002), 064605.

[25] A. Saunders, S. Høibråten, J. J. Kraushaar, B. J. Kriss, R. J. Peterson, R. A. Ristinen, J. T. Brack, G. Hofman, E. F. Gibson C. L. Morris, *Phys. Rev.*, **C53**, (1996), 1745.